

Supplementary Information for:  
A dynamic model of excitation-contraction coupling during  
acidosis in cardiac ventricular myocytes

Edmund J. Crampin<sup>1</sup>

Nicolas P. Smith

<sup>1</sup>Corresponding author. Address: Bioengineering Institute, The University of Auckland, Private Bag 92019, Auckland, New Zealand. Tel.: +64 9 373 7599 ext. 88168, Fax.: +64 9 367 7157, email: e.crampin@auckland.ac.nz

In this supplementary information we give further details of the modifications made to the Luo Rudy dynamic (LRd) model used to simulate the effects of acidosis in cardiac myocytes.

## Acid-Equivalent Transport in the Myocyte

Kinetic models for the four sarcolemmal acid-equivalent transporters were developed using six-state schemes, shown in Fig. S-1. The development of kinetic models for these transporters allows us: (i) to distinguish the relative effects of respiratory acidosis (where extracellular  $\text{CO}_2$  diffuses across the membrane, inducing a drop in intracellular pH) versus intracellular metabolic acidosis (intracellular accumulation of protons); (ii) to represent the relative action of extracellular and intracellular pH on transporter flux (this coupling has been shown to fundamentally affect the pH transient on either side of the membrane (1)) and (iii) to determine the effect on acid transport of changing concentrations of the other ligands:  $\text{HCO}_3^-$ ,  $\text{Cl}^-$  and, in particular, the elevated intracellular  $\text{Na}^+$  that occurs during acidosis due to proton-coupled  $\text{Na}^+$  transport (2).

Here we derive the steady-state fluxes, using rapid equilibrium assumptions for ion binding and unbinding. For simplicity we assume ligand dissociation constants to be equal on each side of the membrane, although this is not a necessary assumption for the following analysis. Transitions between intracellular and extracellular-facing conformations of the protein are assumed to take place on a slower timescale than ion binding and unbinding events. NBC is modelled as a compulsory-order cotransporter, Fig. S-1(a). At thermodynamic equilibrium, each transition between states of the transport cycle must be in equilibrium (detailed balance, see Hill (3) for example).

$$k_i^+ S_i = k_i^- S_{i+1} \quad (\text{S-1})$$

where the  $S_i$  are state occupancy probabilities (which can be interpreted as the fraction of time the transporter is in each state) and  $k_i^+$  and  $k_i^-$  are the rates of transition between the  $i$ th and  $i + 1$ th states, clockwise and anti-clockwise, respectively. In this case, using the rapid binding approximation

$$\frac{[A]_e}{K_{A_e}} S_1 = S_2 \quad \frac{[B]_e}{K_{B_e}} S_2 = S_3 \quad k_2^+ S_3 = k_2^- S_4 \quad (\text{S-2})$$

$$S_4 = \frac{[B]_i}{K_{B_i}} S_5 \quad S_5 = \frac{[A]_i}{K_{A_i}} S_6 \quad k_1^+ S_6 = k_1^- S_1 \quad (\text{S-3})$$

where  $K_{A_i}$  and  $K_{A_e}$  are the intra- and extra-cellular dissociation constants for A, and so forth. Multiplying these expressions we find

$$\prod_{i=1}^6 k_i^+ S_i = \prod_{i=1}^6 k_i^- S_{i+1} \quad (\text{S-4})$$

where  $S_7 \equiv S_1$ , and thus detailed balance requires

$$\frac{k_1^+ k_2^+ \frac{[A]_e}{K_{A_e}} \frac{[B]_e}{K_{B_e}}}{k_1^- k_2^- \frac{[A]_i}{K_{A_i}} \frac{[B]_i}{K_{B_i}}} = \frac{\prod_{i=1}^6 S_i}{\prod_{i=1}^6 S_i} = 1 \quad (\text{S-5})$$

At thermodynamic equilibrium the free energy change of the transport cycle is zero, thus intra- and extra-cellular concentrations of each of the transported ions must be equal, and

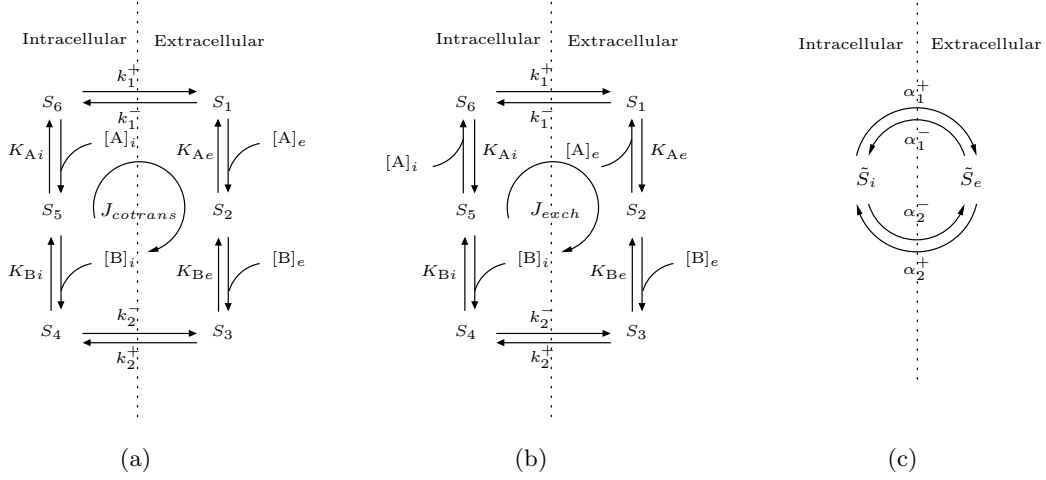


Figure S-1: Schematic diagrams for six-state compulsory order (a) cotransporter (NBC) and (b) exchanger (NHE, CHE, AE). A simplified, two-state cycle is shown in figure (c). For the cotransporter (a), NBC has  $A = \text{Na}^+$  and  $B = \text{HCO}_3^-$ , while for the three exchangers (b), NHE has  $A = \text{H}^+$  and  $B = \text{Na}^+$ , for CHE  $A = \text{OH}^-$  and  $B = \text{Cl}^-$  and for AE  $A = \text{HCO}_3^-$  and  $B = \text{Cl}^-$ .

if we make the simplifying assumption that intra- and extra-cellular dissociation constants are equal, then

$$k_1^+ k_2^+ = k_1^- k_2^- \quad (\text{S-6})$$

Thus from thermodynamic considerations only three of these four rate constants can be specified independently.

The transport flux can be determined using the rapid equilibrium approximation to simplify the transporter cycle kinetics. Assuming rapid binding, the three states representing intra- and extra-cellular facing conformations can be collapsed, giving

$$S_1 + S_2 + S_3 \equiv \tilde{S}_e = \left(1 + \frac{[A]_e}{K_A} + \frac{[A]_e [B]_e}{K_A K_B}\right) S_1 \quad (\text{S-7})$$

$$= \left(1 + \frac{K_B}{[B]_e} + \frac{K_A K_B}{[A]_e [B]_e}\right) S_3 \quad (\text{S-8})$$

$$S_4 + S_5 + S_6 \equiv \tilde{S}_i = \left(1 + \frac{K_B}{[B]_i} + \frac{K_A K_B}{[A]_i [B]_i}\right) S_4 \quad (\text{S-9})$$

$$= \left(1 + \frac{[A]_i}{K_A} + \frac{[A]_i [B]_i}{K_A K_B}\right) S_6 \quad (\text{S-10})$$

(for further details of this model simplification, see Smith and Crampin (4)) and hence the kinetics are equivalent to a two-state model,  $\tilde{S}_i$ ,  $\tilde{S}_e$ , Fig. S-1(c), with clockwise transition rates  $\alpha_{1,2}^+$  and anti-clockwise rates  $\alpha_{1,2}^-$  which are functions of the ionic concentrations:

$$\alpha_1^+(A)_i, [B]_i = q \frac{k_1^+ K_A K_B}{K_A K_B + K_B [A]_i + [A]_i [B]_i}, \quad \alpha_1^-(A)_e, [B]_e = \frac{k_1^- K_A K_B}{K_A K_B + K_B [A]_e + [A]_e [B]_e} \quad (\text{S-11})$$

$$\alpha_2^+(A)_e, [B]_e = \frac{k_2^+ [A]_e [B]_e}{K_A K_B + K_B [A]_e + [A]_e [B]_e}, \quad \alpha_2^-(A)_i, [B]_i = \frac{k_2^- [A]_i [B]_i}{K_A K_B + K_B [A]_i + [A]_i [B]_i} \quad (\text{S-12})$$

At steady state

$$\tilde{S}_e = 1 - \tilde{S}_i = \frac{\alpha_1^+ + \alpha_2^-}{\alpha_1^+ + \alpha_1^- + \alpha_2^+ + \alpha_2^-} \quad (\text{S-13})$$

and hence the steady-state transport flux  $J_{cotrans}$  is

$$J_{cotrans}([A]_i, [A]_e, [B]_i, [B]_e) = \alpha_1^+ \tilde{S}_i - \alpha_1^- \tilde{S}_e \quad (\text{S-14})$$

$$= \frac{\alpha_1^+ \alpha_2^+ - \alpha_1^- \alpha_2^-}{\alpha_1^+ + \alpha_1^- + \alpha_2^+ + \alpha_2^-} \quad (\text{S-15})$$

Alternatively, the steady-state flux can be derived using Hill's diagram method (3).

The three other transporters, NHE, CHE and AE are modelled as compulsory order exchangers. Steady-state transport flux for the compulsory order exchanger (Fig. S-1(b)) may be derived using the same approach, yielding the same thermodynamic constraint on the rate constants for conformational change of the protein. The rapid equilibrium assumption reduces the model to a two-state cycle (Fig. S-1(c)) with state transition rates

$$\beta_1^+(A)_i, [B]_i) = \frac{k_1^+ K_B [A]_i}{K_A K_B + K_B [A]_i + K_A [B]_i} \quad \beta_1^-(A)_e, [B]_e) = \frac{k_1^- K_B [A]_e}{K_A K_B + K_B [A]_e + K_A [B]_e} \quad (\text{S-16})$$

$$\beta_2^+(A)_e, [B]_e) = \frac{k_2^+ K_A [B]_e}{K_A K_B + K_B [A]_e + K_A [B]_e} \quad \beta_2^-(A)_i, [B]_i) = \frac{k_2^- K_A [B]_i}{K_A K_B + K_B [A]_i + K_A [B]_i} \quad (\text{S-17})$$

and the steady-state exchanger flux  $J_{exch}$  is given by the equation

$$J_{exch}([A]_i, [A]_e, [B]_i, [B]_e) = \frac{\beta_1^+ \beta_2^+ - \beta_1^- \beta_2^-}{\beta_1^+ + \beta_1^- + \beta_2^+ + \beta_2^-} \quad (\text{S-18})$$

Experimental data on the cotransporter flux  $J_{nbc}$  and three exchanger fluxes  $J_{nhe}$ ,  $J_{che}$  and  $J_{ae}$  were fitted to these expressions along with allosteric modulation of the fluxes by intra- and extra-cellular pH, as given by Eq. 15–18, respectively.

**Allosteric Regulation:** Where appropriate we have incorporated allosteric regulation of the transport fluxes by protons, at intracellular and extracellular binding sites, according to available  $\text{pH}_i$  and  $\text{pH}_e$  data. We assumed that proton dissociation constants for allosteric sites are independent of the conformation of the protein, and hence these allosteric interactions modulate the effective proportion of available transporters.

**Parameter Estimation:** Parameters for the four acid-equivalent transporters were estimated using a sequential quadratic programming algorithm (5) to optimise the model fit to  $\text{pH}_i$ -dependence data, measured by Leem et al. (6), along with whole-cell steady-state  $\text{pH}_i$  and  $\text{pH}_e$  data from Vaughan-Jones and Spitzer (1). Use of these whole-cell data requires that the parameters for the transporters be fitted simultaneously.

Firstly, we used data from Leem et al. (6), Ch'en and Vaughan-Jones (7) and van Borren et al. (8) to fit intra and extracellular concentration dependence of  $J_{nbc}$ , independently of the other transporter models. Specifically the  $\text{pH}_i$  dependence was defined by the data of Leem et al. (6) who pharmacologically inhibited NHE and then induced an intracellular acid load by ammonium prepulse at a 5%  $\text{CO}_2$  partial pressure ( $P_{\text{CO}_2}$ ). To fit NBC flux data,  $\text{pH}_i$ ,  $\text{pH}_e$ , intra and extracellular sodium and intra and extracellular bicarbonate must be defined for each data point. The  $\text{CO}_2$  concentration  $[\text{CO}_2] = \alpha P_{\text{CO}_2}$ , where  $\alpha = 0.03253 \text{ mM mmHg}^{-1}$  is the solubility of  $\text{CO}_2$  (and atmospheric pressure is 760 mmHg). Thus at atmospheric pressure, a partial pressure of 5%  $\text{CO}_2$  corresponds to a concentration of 1.236 mM. From the  $\text{CO}_2$  hydration reaction (see below), at equilibrium in the extracellular space

$$[\text{HCO}_3^-]_e = [\text{CO}_2]_e 10^{\text{pH}_e - \text{pK}_a}. \quad (\text{S-19})$$

CO<sub>2</sub> diffuses across the cell membrane so, at equilibrium, [HCO<sub>3</sub><sup>-</sup>]<sub>i</sub> can be calculated from:

$$[\text{HCO}_3^-]_i = [\text{HCO}_3^-]_e 10^{\text{pH}_i - \text{pH}_e} \quad (\text{S-20})$$

where pKa for CO<sub>2</sub> hydration is 6.12 at 37°C. Thus at equilibrium when pH<sub>i</sub> and pH<sub>e</sub> are 7.1 and 7.4, respectively, bicarbonate concentrations are approximately 12 mM ([HCO<sub>3</sub><sup>-</sup>]<sub>i</sub>) and 22 mM ([HCO<sub>3</sub><sup>-</sup>]<sub>e</sub>). Thus from Eq. S-19 the change in [HCO<sub>3</sub><sup>-</sup>]<sub>i</sub> can be determined as pH<sub>i</sub> is altered. The dependence of NBC flux on pH<sub>e</sub> and extracellular sodium was defined with the data of Ch'en and Vaughan-Jones (7). In this study NBC flux was measured after a 15 mM ammonium prepulse (assumed in the model to reduce intracellular pH<sub>i</sub> to 6.7) over a range of extracellular sodium concentrations reporting a V<sub>max</sub> of 2.07 mM min<sup>-1</sup> and a Hill coefficient of 0.97. The pH<sub>e</sub> dependence was measured by altering ([HCO<sub>3</sub><sup>-</sup>]<sub>e</sub>) from 2 to 60 mM which in turn varies pH<sub>e</sub> (see Eq. S-20) while setting [HCO<sub>3</sub><sup>-</sup>]<sub>i</sub> constant using 3% CO<sub>2</sub>. Finally the reported reduction in NBC flux to zero at pH<sub>e</sub> of 6.4 (8) was introduced as an additional data point in the model fit. Intracellular Na<sup>+</sup>, while not stated in this study, was assumed to be at the normal resting values for the myocyte of 12.23 mM in all of these studies and [Na<sup>+</sup>]<sub>e</sub> was set at 140.4 mM when not explicitly varied. The model NBC flux was fitted simultaneously using data from these three sources and the model fit with experimental data is shown in Fig. 5 and in Fig. S-2(a)-(b). Model parameters are listed in the first column of Table 3.

Following fitting of the NBC model, parameters for NHE, CHE and AE were fitted simultaneously. Intracellular pH dependence was defined once again using the data of Leem et al. (6), with intra and extracellular chloride concentrations, again not reported, and thus assumed to be at resting myocyte levels of 20.0 and 126.0 mM respectively (9). The Hill coefficient of allosteric intracellular regulation was constrained in the fitting process, as proposed by Vaughan-Jones and Spitzer (1). The extracellular inhibition of NHE to 60% of its resting flux at a pH<sub>e</sub> of 6.4 (8) was included as an additional data point. The extracellular pH dependence of all NHE, CHE and AE was constrained using the steady-state relationship reported by Sun et al. (10) and Vaughan-Jones and Spitzer (1). From these data a linear gradient of 0.35 pH<sub>i</sub> units per unit change in pH<sub>e</sub> was reported at steady state over a range of pH<sub>e</sub> values in both CO<sub>2</sub> free solution (where only NHE and CHE) are active and in the presence of 5 % CO<sub>2</sub> buffers (when all four transporters are active). The model fit to this steady-state relationship in CO<sub>2</sub>-free solution is shown in Fig. S-2(c) which constrains the relationship between NHE and CHE over the range of pH changes. Figure S-2(d) shows the model fitted to experimental data where the data have been shifted to accommodate the equilibrium values defined by the intracellular pH-dependent data of Leem et al. (6) (this experimental variation is acknowledged in the original data (1)). For all fits, Na<sup>+</sup> and Cl<sup>-</sup> values were unchanged from the resting cellular concentrations used above. In both cases the the gradient of 0.35 pH<sub>i</sub>/pH<sub>e</sub> is maintained in the model and Fig. 5 demonstrates excellent fits to the intracellular pH<sub>i</sub>-dependent data. The full list of parameters for each of the transporters is given in Table 3.

## Ca<sup>2+</sup> Buffering

In order to determine the total calcium in the cell, required for the charge-balance calculation of membrane potential, we need to know buffered calcium concentration. We

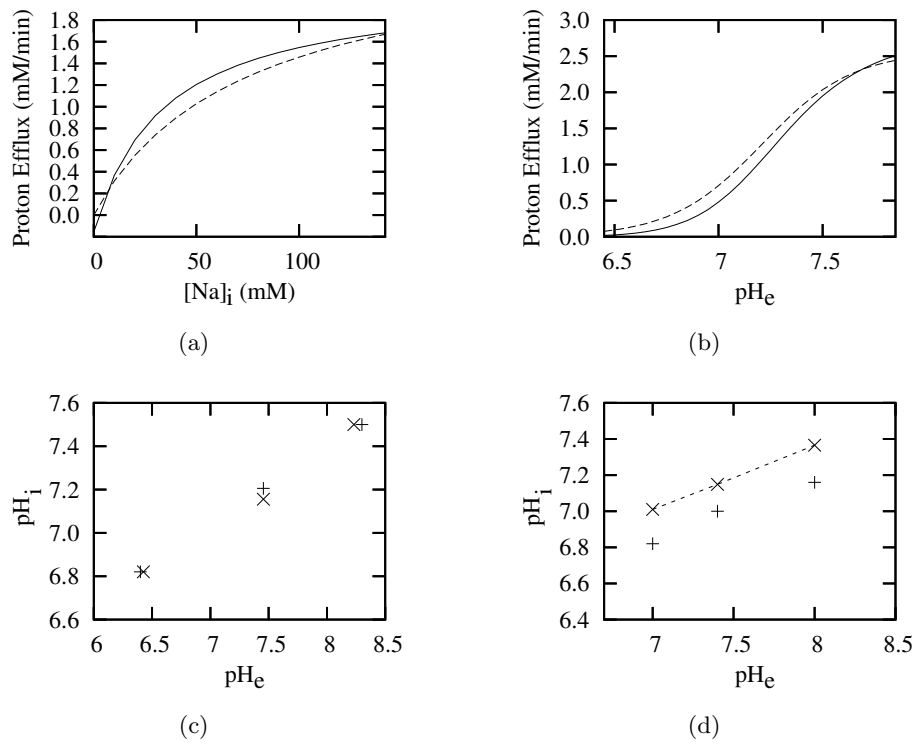


Figure S-2: (a) Model (solid) and experimental fit (7) (dashed)  $[Na^+]_e$ -dependence of NBC flux. (b) Model (solid) and experimental fit (7) (dashed)  $pH_e$ -dependence of NBC flux. (c) Model (+) and experimentally measured (1) ( $\times$ ) steady-state relationship between  $pH_i$  and  $pH_e$  in  $CO_2$  free buffer. (d) Model (+), experimentally measured (1) ( $\times$ ) and adjusted (dashed) experimental fit to steady-state relationship between  $pH_i$  and  $pH_e$  in 5%  $CO_2$  buffer.

calculate calcium buffering explicitly, assuming steady-state buffering, according to

$$[\text{Ca}^{2+}]_B = \overline{[\text{Ca}^{2+}]}_B \frac{[\text{Ca}^{2+}]}{K_M^B + [\text{Ca}^{2+}]} \quad (\text{S-21})$$

where  $B$  is the buffer Troponin (*trpn*), Calmodulin (*cmdn*) or Calsequestrin (*csqn*),  $\overline{[\text{Ca}^{2+}]}_B$  is the maximum calcium buffering on  $B$  (i.e. total concentration of  $B$ ) and  $[\text{Ca}]$  is the free calcium concentration in the appropriate compartment (cytosol and junctional SR (*jsr*) respectively). Buffering strength,  $\beta_{\text{Ca}}$ , defined by

$$\frac{d[\text{Ca}]}{dt} = J \cdot \frac{1}{\beta_{\text{Ca}}} \quad (\text{S-22})$$

where  $J$  is the net inward flux of calcium into the compartment, is given by

$$\beta_{\text{Ca}} = 1 + \sum_B \overline{[\text{Ca}^{2+}]}_B \frac{K_M^B}{(K_M^B + [\text{Ca}^{2+}])^2} \quad (\text{S-23})$$

where the sum is over all buffers present in the compartment.

### Initial Conditions

Initial conditions which provide stable concentrations on a beat-to-beat basis for the LRd model with modifications outlined above at a 500 ms cycle length are given in Table 1. Initially,  $\text{CO}_2$  is assumed to be equilibrated across the cell membrane (at 5%  $\text{CO}_2$ , which is equivalent to a concentration of 1.236 mM), and the  $\text{CO}_2$  hydration reaction is assumed to be at equilibrium on either side of the membrane (which, given initial  $\text{pH}_i$  and  $\text{pH}_e$ , determines the initial intra- and extra-cellular bicarbonate concentrations, 13.4 mM and 23.6 mM, respectively).

Description	Units	Symbol	Value
Membrane potential	mV	$E_m$	$-0.6955 \times 10^2$
Intracellular pH		$\text{pH}_i$	$0.7150 \times 10^1$
Extracellular pH		$\text{pH}_e$	$0.7400 \times 10^1$
CO <sub>2</sub> concentration	mM	$[\text{CO}_2]$	$0.1236 \times 10^1$
Intracellular Na <sup>+</sup> concentration	mM	$[\text{Na}^+]_i$	$0.1267 \times 10^2$
Intracellular K <sup>+</sup> concentration	mM	$[\text{K}^+]_i$	$0.1308 \times 10^3$
Intracellular Cl <sup>-</sup> concentration	mM	$[\text{Cl}^-]_i$	$0.2174 \times 10^2$
Intracellular Ca <sup>2+</sup> concentration	mM	$[\text{Ca}^{2+}]_i$	$0.1466 \times 10^{-3}$
Junctional SR Ca <sup>2+</sup> concentration	mM	$[\text{Ca}^{2+}]_{j\text{sr}}$	$0.9918 \times 10^0$
Network SR Ca <sup>2+</sup> concentration	mM	$[\text{Ca}^{2+}]_{\text{nsr}}$	$0.2271 \times 10^1$
Na <sup>+</sup> channel $E_m$ -dependant activation		$m$	$0.1506 \times 10^{-1}$
Na <sup>+</sup> channel $E_m$ -dependant inactivation		$h$	0.9882
Na <sup>+</sup> channel $E_m$ -dependant inactivation		$j$	0.9929
L-type Ca <sup>2+</sup> channel $E_m$ -dependant activation		$d$	$0.1320 \times 10^{-4}$
L-type Ca <sup>2+</sup> channel $E_m$ -dependant inactivation		$f$	0.9992
Slowly Activating K <sup>+</sup> time-dependant activation		$x_{s1}$	$0.1894 \times 10^{-1}$
Slowly Activating K <sup>+</sup> time-dependant activation		$x_{s2}$	$0.6440 \times 10^{-1}$
Rapidly Activating K <sup>+</sup> time-dependant activation		$x_r$	$0.1902 \times 10^{-3}$
T-type Ca <sup>2+</sup> Channel $E_m$ -dependant activation		$b$	$0.1234 \times 10^{-2}$
T-type Ca <sup>2+</sup> Channel $E_m$ -dependant inactivation		$g$	0.9781
$I_{to}$ Current activation		$zdv$	$0.1209 \times 10^{-1}$
$I_{to}$ Current inactivation		$ydv$	1.000
Proportion of available Actin sites		$z$	$0.2463 \times 10^{-4}$

Table 1: Initial conditions for pacing at 500 ms intervals.



## References

1. Vaughan-Jones, R. D., and K. W. Spitzer. 2002. Role of bicarbonate in the regulation of intracellular pH in the mammalian ventricular myocyte. *Biochem. Cell. Biol.* 80:579–596.
2. Allen, D. G., and X. H. Xiao. 2003. Role of the cardiac  $\text{Na}^+/\text{H}^+$  exchanger during ischemia and reperfusion. *Cardiovasc. Res.* 57:934–941.
3. Hill, T. L. 1989. *Free Energy Transduction and Biochemical Cycle Kinetics*. Springer, New York.
4. Smith, N. P., and E. J. Crampin. 2004. Development of models of active ion transport for whole-cell modelling: Cardiac sodium-potassium pump as a case study. *Prog. Biophys. Mol. Biol.* 85:387–405.
5. Gill, P. E., W. Murray, M. A. Saunders, and M. H. Wright. 1984. Procedures for optimization problems with a mixture of bounds and general linear constraints. *ACM Transactions on Mathematical Software* 10:282–298.
6. Leem, C. H., D. Lagadic-Gossmann, and R. D. Vaughan-Jones. 1999. Characterization of intracellular pH regulation in the guinea-pig ventricular myocyte. *J. Physiol.* 517:159–180.
7. Ch'en, F. F.-T., and R. D. Vaughan-Jones. 2001.  $\text{Na}^+/\text{HCO}_3^-$  co-transport is instructed by pH and not bicarbonate or  $\text{Na}^+$ . *Biophys. J.* 80:74.
8. van Borren, M. M., A. Baartscheer, R. Wilders, and J. H. Ravesloot. 2004. NHE-1 and NBC during pseudo-ischemia/reperfusion in rabbit ventricular myocytes. *J. Mol. Cell Cardiol.* 37:567–77.
9. Vaughan-Jones, R. D. 1986. An investigation of chloride-bicarbonate exchange in the sheep cardiac Purkinje fibre. *J. Physiol.* 379:377–406.
10. Sun, B., L. C. H., and R. D. Vaughan-Jones. 1996. Novel chloride-dependent acid loader in the guinea-pig ventricular myocyte: part of a dual acid-loading mechanism. *J. Physiol.* 495:65–82.